

## COMPLEXES OF FUNCTIONALIZED QUANTUM DOTS AND CHLORIN $e_6$ IN PHOTODYNAMIC THERAPY

R. Rotomskis <sup>a,b</sup>, J. Valanciunaite <sup>b</sup>, A. Skripka <sup>b</sup>, S. Steponkiene <sup>b</sup>, G. Spogis <sup>b</sup>,  
S. Bagdonas <sup>a</sup>, and G. Streckyte <sup>a</sup>

<sup>a</sup>*Biophotonics Laboratory, Laser Research Center, Vilnius University, Saulėtekio 9-III, LT-10222 Vilnius, Lithuania*  
E-mail: giedre.streckyte@ff.vu.lt

<sup>b</sup>*Biomedical Physics Laboratory, Institute of Oncology of Vilnius University, Baublio 3b, LT-08406 Vilnius, Lithuania*

Received 11 December 2012; accepted 20 December 2012

Recently, it has been suggested that quantum dots (QDs) could be used in the photodynamic therapy of cancer as resonance energy donors for conventional porphyrin type photosensitizers. Here we present the results of the spectroscopic studies on the formation of a non-covalent complex between QDs and photosensitizer chlorin  $Ce_6$  in an aqueous medium and in the presence of bovine serum albumin (BSA). Changes in the absorption and fluorescence spectra of QDs and  $Ce_6$  revealed the formation of a QD- $Ce_6$  complex which occurs due to hydrophobic interaction between the nonpolar moiety of an amphiphilic photosensitizer and the hydrophobic part of the lipid-based coating of the QD. The photosensitizer conjugated with the QD could be indirectly excited by the Forster resonance energy transfer (FRET) from the QD to  $Ce_6$ . The investigation on the capacity of such complex to generate  $^1O_2$  showed that the QD- $Ce_6$  complex irradiated by visible light is able to produce  $^1O_2$  more efficiently than QDs or  $Ce_6$  taken separately. The photoinactivation of cells incubated with the QD- $Ce_6$  complex and irradiated in the spectral region where the photosensitizer does not absorb provided evidence that such complex could induce FRET-mediated cell destruction.

**Keywords:** quantum dots, lipids, photosensitizer, energy transfer, photodynamic therapy

**PACS:** 87.64.kv, 87.85Rs

### 1. Introduction

Innovative technologies based on application of nanoparticles are developed to bring new solutions for fighting oncological diseases. One of the developing methods introduced into clinical practice about twenty years ago is photodynamic therapy (PDT), a minimally invasive therapeutic modality presently approved for treatment of several types of cancer and non-oncological disorders. The action of PDT is based on the common use of a compound with photosensitising properties selectively accumulated in malignant tissues and the visible light, preferentially in the red region of the spectrum where tissues are more permeable to light. The aim is to bring about a cytotoxic effect to cancerous tissue: a photosensitizer of negligible dark toxicity accumulated preferentially in rapidly

dividing cells is activated by light and elicits the toxic action. Upon illumination, the photosensitizer (PS) is excited from the ground state ( $S_0$ ) to the first excited singlet state ( $S_1$ ) followed by conversion to the triplet state ( $T_1$ ) via intersystem crossing. The excited triplet state may react in two ways, defined as type I and type II mechanisms. A type I mechanism involves hydrogen-atom abstraction or electron-transfer reactions between the excited state of the sensitizer and a substrate to yield free radicals and radical ions which can cause irreparable biological damage. A type II mechanism results from the energy transfer between the excited triplet state of the sensitizer and the ground state molecular oxygen generating the first excited state of oxygen, singlet oxygen ( $^1O_2$ ). This species is extremely reactive and can interact with a large number of biological substrates,

inducing oxidative damage and, ultimately, cell inactivation. Singlet oxygen is generally accepted as the major damaging species in PDT [1] and, therefore, photosensitization typically does not occur in anoxic areas of tissue.

Chlorin  $e_6$  ( $Ce_6$ ) is a second-generation PS with a high quantum yield of singlet oxygen production of 0.65 at pH 7–8 [2]. In addition, the amphiphilic structure of a  $Ce_6$  molecule allows easy penetration through cell membrane, thus ensuring effective accumulation inside cells [3, 4]. However,  $Ce_6$  is highly unstable under light exposure and its absorbance at the red side of the visible spectrum is insufficient for effective excitation in greater depths of the tissue. Another important factor determining the efficacy of PDT is selectivity of PS localization in the tumour, i. e. high ratios of sensitizer concentration in the tumour to that in the healthy surrounding tissue should be achieved. To address these problems new PSs are being sought together with the improved delivery system, including nanoparticle-based carrier systems.

Nanoparticles, such as semiconductor quantum dots (QDs), are gaining much attention due to their unique size-dependent optical properties, high stability, and easy surface modification by binding different functional groups and biomolecules, and are considered promising materials for many biological and medical applications. Recently, it is proposed to use QDs not only for diagnostic purposes but also in the PDT of cancer [5, 6]. Since QDs themselves were shown to generate singlet oxygen inefficiently [5], it has been suggested to use QDs in PDT as resonance energy donors for a conventional PS. The complexation of QDs with a PS could broaden the excitation range of the PS and enhance their excitation efficiency as well as solve selectivity problems of a conventional PS in PDT, thus greatly enhancing its applicability and efficiency.

The nature of interaction between QDs and PSs is crucial for the stability, photophysical properties and effectiveness of the QD-PS complex. Numerous studies on the primary photo-physical properties of complexes of QDs and various PSs in aqueous solutions assembled mainly by the electrostatic interaction have been already performed [7–9]; however, the stability, compatibility in biological media and singlet oxygen generation of these complexes is yet to be investigated.

In this work, we present steady-state spectroscopic studies on the formation of a non-covalent complex between QDs with lipid coatings and amphiphilic photosensitizer  $Ce_6$ . The excitation of  $Ce_6$  via FRET by exploring non-covalent complexation of the PS with QDs was studied and generation of  $^1O_2$  by such complex was measured. The possibility of a QD- $Ce_6$  complex as a candidate for the photosensitized tumour therapy was evaluated as well.

## 2. Materials and methods

### 2.1. Reagents and preparation of solutions

Chlorine  $e_6$  tetrasulfonic acid ( $Ce_6$ ) was purchased from *Frontier Scientific Inc.* (USA). CdSe/ZnS QDs with terminal amine or carboxyl groups (620 nm), used for the investigations of the formation of a QD- $Ce_6$  complex, were obtained from *eBioscience* (USA).

The stock solution of  $Ce_6$  was freshly prepared and further diluted to concentrations from 0.005 to 5  $\mu$ M. QDs solutions were prepared by diluting aqueous stock solution (10.9 nmol/ml) provided directly by manufacturers. Mixture solutions of QDs with  $Ce_6$  were prepared by adding 1  $\mu$ l of  $Ce_6$  solution of appropriate concentration to 2 ml of the QDs solution. In these mixed QD- $Ce_6$  solutions, the concentration of QDs was kept constant at 0.05  $\mu$ M, while concentration of  $Ce_6$  varied from 0.025 to 5  $\mu$ M (QDs: $Ce_6$  molar ratios from 1:0.5 to 1:100 were obtained). The spectra were measured 15 minutes after the preparation of QD- $Ce_6$  mixture solutions.

CdSe/ZnS QDs coated with amphiphilic polymer (AMP) and polyethylene glycol (PEG) bearing amine groups ( $NH_2$  100%), used for the investigations of the formation of a QD- $Ce_6$  complex in an aqueous medium in the presence of bovine serum albumin, were obtained from *Invitrogen Corp.* (USA). Bovine serum albumin (BSA) was purchased from *Sigma* (Germany).

The stock solutions of  $Ce_6$  and BSA were freshly prepared before experiments. The QDs solution (0.05  $\mu$ M) was prepared by directly diluting the stock solution of QDs (8  $\mu$ M) provided by manufacturers. For the spectroscopic experiments three working solutions with a different mixing order of QDs,  $Ce_6$  and BSA were used. The appropriate

amount of BSA or  $Ce_6$  was added to QDs solutions to reach the molar ratio 1:20 for QDs:BSA and 1:10 for QDs: $Ce_6$ . The solution initially containing  $Ce_6$  ( $0.5 \mu\text{M}$ ) was mixed with BSA to the molar ratio of 10:20. Further, appropriate amounts of  $Ce_6$ , BSA, and QDs solutions were added to QD-BSA, QD- $Ce_6$ , and  $Ce_6$ -BSA mixtures, respectively, to reach the final molar ratio of all three components QD-BSA- $Ce_6$  in the mixture solutions to be 1:20:10.

CdSe/ZnS QDs (625 nm) in toluene ( $15.18 \mu\text{M}$ ), used for the elucidation of the effect of lipid coating on the formation of a QD- $Ce_6$  complex, were purchased from *Evident Tech.* (USA). Phospholipids containing saturated and unsaturated fatty acids: 1,2-dipalmitoyl-*sn*-glycero-3-phosphoethanolamine-N-[methoxy(polyethylene glycol)-2000] (ammonium salt) (PEG-DPPE), 1,2-dioleoyl-*sn*-glycero-3-phosphoethanolamine-N-[methoxy(polyethylene glycol)-2000] (ammonium salt) (PEG-DOPE), and 1,2-dioleoyl-*sn*-glycero-3-phosphocholine (DOPC), were obtained from *Avanti Polar Lipids* (USA).

Carboxyl-Functionalized eFluor® 605NC QDs, composed of CdSe/ZnS core/shell, outer lipid coating with PEG and carboxyl functional groups and used for the evaluation of the production of singlet oxygen by a QD- $Ce_6$  complex as well as in PDT experiments in cells, were purchased from *eBioscience* (USA). Singlet oxygen sensor green (SOSG) was obtained from *Invitrogen* (USA). All materials were used without further purification. Solutions were prepared in the phosphate buffer (PB) solution of pH 7.

## 2.2. Spectroscopic measurements

Absorption measurements were carried out with the Cary 50 spectrophotometer (*Varian Inc.*, USA). Fluorescence measurements were performed on the Cary Eclipse fluorescence spectrophotometer (*Varian Inc.*, USA). Quartz cuvette with the optical path length of 1 cm was used for absorption and fluorescence measurements.

## 2.3. Evaluation of singlet oxygen production by QD- $Ce_6$ complex

The stock solution of CdSe/ZnS (605 nm) QDs bearing lipid-based coating with terminal amine

groups was diluted to the concentration of  $0.02 \mu\text{M}$ . The stock solution of  $Ce_6$  was prepared just before the experiments and further diluted to the working  $0.2 \mu\text{M}$   $Ce_6$  concentration. Mixed QD- $Ce_6$  solutions were prepared by adding  $5 \mu\text{l}$   $Ce_6$  solution of appropriate concentration to 2 ml of QDs solutions. The final concentration of QDs in the QD- $Ce_6$  mixture solution was  $0.02 \mu\text{M}$ , while  $Ce_6$  concentration was  $0.2 \mu\text{M}$  (the QDs: $Ce_6$  molar ratio 1:0.1 was obtained). For  $^1\text{O}_2$  detection,  $2 \mu\text{l}$  of SOSG stock solution was added to QDs,  $Ce_6$ , and QD- $Ce_6$  solutions. The final concentration of SOSG was  $2 \mu\text{M}$  in all used solutions.

The irradiation of 2 ml QDs,  $Ce_6$ , or QD- $Ce_6$  solutions was performed using a continuous 402 nm light source ( $P = 45 \text{ mW}/\text{cm}^2$ ). Upon irradiation, the magnetic stirring of solutions was performed.

## 2.4. Efficacy of QD- $Ce_6$ complex in PDT

### 2.4.1. Cells

MiaPaCa-2 cells were purchased from the Health Protection Agency Culture Collection. The cells were cultured in Dulbecco's modified Eagle's medium (DMEM), supplemented with 10% foetal bovine serum (FBS), 100 U/ml penicillin, 100 mg/ml streptomycin, and 4 mM L-alanyl-glutamine. The cells were routinely cultivated in  $25 \text{ cm}^2$  culture dishes under standard conditions by subculturing them 2–3 times a week and keeping in a humidified incubator at  $37^\circ\text{C}$ .

### 2.4.2. Preparation of QD- $Ce_6$ complex solution

In QD- $Ce_6$  mixture solutions the concentration of QDs was  $0.02 \mu\text{M}$ , while the concentration of  $Ce_6$  was  $0.1 \mu\text{M}$ , maintaining the molar ratio of QD: $Ce_6$  at 1:5. All measurements were performed 20 minutes after preparation of solutions, allowing the formation of a QD- $Ce_6$  complex.

### 2.4.3. FLIM in live cancer cells

Cells were seeded into an 8-chambered coverglass plate (*Nalge Nunc International*, USA).  $3 \times 10^4$  cells were seeded in each chamber and incubated with the QDs ( $0.2 \mu\text{M}$ ),  $Ce_6$  ( $1 \mu\text{M}$ ), and QD- $Ce_6$  (molar ratio 1:5) complex in PBS (supplemented with  $\text{Ca}^{2+}$  and  $\text{Mg}^{2+}$ ). After 2 h of incubation the old medium was carefully aspirated, the cells were washed twice with PBS and supplemented with

fresh PBS. The cellular uptake of the QD-Ce<sub>6</sub> complex was assessed using the Nikon Eclipse Te2000-U (Japan) microscope with the confocal laser scanning system C1si (capable of 32 bit spectral imaging) equipped with the CO<sub>2</sub> microscope stage incubation system (*OkoLab*, Italy). Measurements were done using a 60×/1.4 NA oil immersion objective. The lifetime imaging was done using the Lifetime and FCS Upgrade (*PicoQuant GmbH*, Germany) for Nikon C1si. The system consisted of a 404 nm pulse diode laser with a pulse width of 39 ps and repetition rate of 10 MHz. The reflected fluorescence signal was filtered by a 650±75 nm filter. The detected photons were captured by a photomultiplier tube (PMT) and photons were counted by a time correlated single-photon counter PicoHarp 300 (*PicoQuant GmbH*, Germany). Initialization, scanning, and acquisition were controlled by the same Nikon C1si microscope system.

#### 2.4.4. Photosensitizing properties of QD-Ce<sub>6</sub> complex

Cells were seeded into 96 well plates, 50,000 cells per well. After 24 hours the medium was replaced with 100 μl DPBS containing a QD-Ce<sub>6</sub> complex and left for 3.5 hours in the incubator (in the dark).

For the irradiation procedure, cells were transferred to the microscope stage incubation system and exposed to 25 mW/cm<sup>2</sup> irradiation at 470 nm, applied for 15 minutes on each well, giving a dose of 15 J/cm<sup>2</sup>. Photosensitizing properties were evaluated as a capacity of the QD-Ce<sub>6</sub> complex to induce obvious cell death.

### 3. Results

#### 3.1. Formation of QD-Ce<sub>6</sub> complex

The absorption spectra of CdSe/ZnS QDs (620 nm) bearing amine groups and also Ce<sub>6</sub> in aqueous solution at pH 7 are shown in Fig. 1(a). The absorption spectrum of free Ce<sub>6</sub> consists of the intensive Soret band at 403 nm and four weaker Q bands with the most intensive Q(I) in the red spectral side at 655 nm. The absorption spectrum of QDs decreases towards the red spectral side and ends with an exciton peak at around 600 nm. The absorption spectra of mixed QD-Ce<sub>6</sub> solutions did not display a simple superposition of QDs and Ce<sub>6</sub> spectra at corresponding concentrations of both components. Various absorption spectral changes were observed in QD-Ce<sub>6</sub> mixture solutions

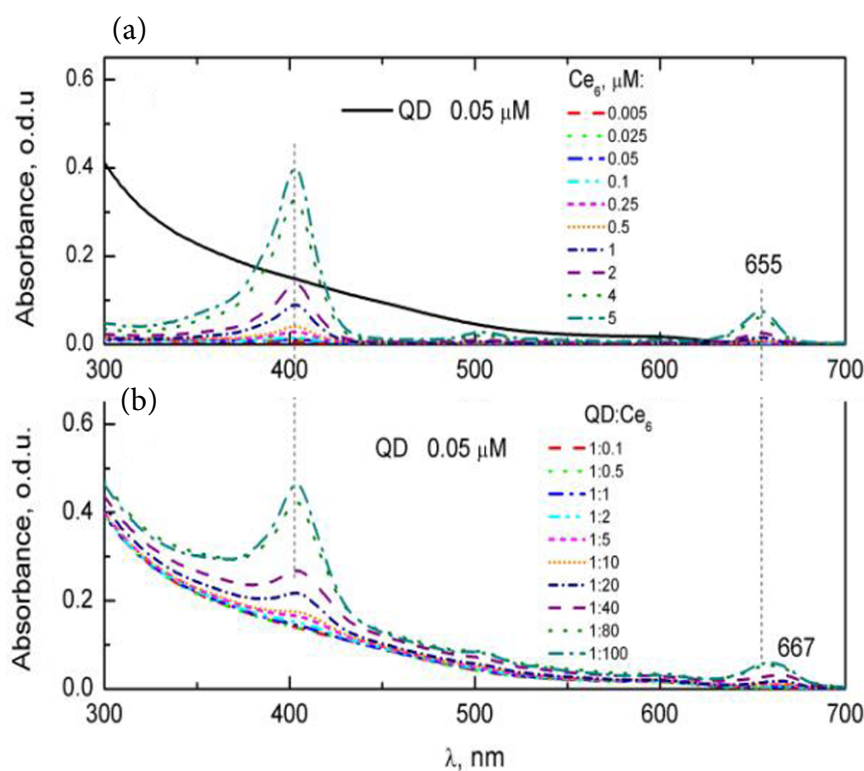


Fig. 1. (a) Absorption spectrum of QDs (0.05 μM) and spectra of various solutions of Ce<sub>6</sub>. (b) Absorption spectra of mixed QD-Ce<sub>6</sub> solutions at various QD:Ce<sub>6</sub> molar ratios.

upon increase of  $Ce_6$  concentration, keeping QDs concentration constant (Fig. 1(b)). The most pronounced changes were observed in the region of the  $Ce_6$  Q(I) band, which underwent a bathochromic shift to 667 nm. However, at the highest added  $Ce_6$  amounts (QD: $Ce_6$  molar ratios 1:80–1:100), an absorption band of free  $Ce_6$  (655 nm) also appeared. Thus, the peak at 667 nm can be attributed to the formed QD- $Ce_6$  complex.

Similarly, distinct changes in intensity were observed in the fluorescence spectra of mixed QD- $Ce_6$  solutions at different molar ratios of QDs and  $Ce_6$  (Fig. 2). The fluorescence spectra of QD- $Ce_6$  mixture solutions displayed two fluorescence bands at 622 and 670 nm under excitation at 465 nm. The first band belongs to QDs. Since the fluorescence peak of free  $Ce_6$  was detected at 660 nm, the second

band with the peak at 670 nm could be assigned to the bound  $Ce_6$  molecules in the formed QD- $Ce_6$  complex. It has to be noted that this band was detected under excitation, at which the absorbance of QDs prevails and the absorbance of  $Ce_6$  is minimal (Fig. 1(a)).

The intensity of the QDs photoluminescence (PL) band at 622 nm decreased with the changing of a molar ratio between QD and  $Ce_6$  from 1:0.1 to 1:10, while the intensity of the band at 670 nm increased (Fig. 2(a)). However, further increase of relative  $Ce_6$  concentration from 1:20 to 1:100 resulted in intensity decrease through the whole spectrum (Fig. 2(b)). When  $Ce_6$  was excited directly at 400 nm (data not shown), the fluorescence peak of free  $Ce_6$  appeared at 660 nm in the mixed solutions at QD: $Ce_6$  molar ratios exceeding 1:10, and its intensity further increased in contrast to the observed decrease in intensity of the peak at 670 nm for bound  $Ce_6$  molecules.

Both QDs and  $Ce_6$  spectra contributed to the fluorescence excitation spectrum of a QD- $Ce_6$  mixture measured at 670 nm (Fig. 3). The partial intensity of QDs PL in a mixture spectrum was significantly higher than the total intensity of the fluorescence excitation spectrum of a pure QDs solution measured at this emission wavelength. However, the partial intensity of the  $Ce_6$  spectrum remained relatively unchanged.

One might expect that electrostatic interaction between the positively charged amino groups of QDs coating and negatively charged carboxyl groups of  $Ce_6$  might be a pivotal factor for QD- $Ce_6$

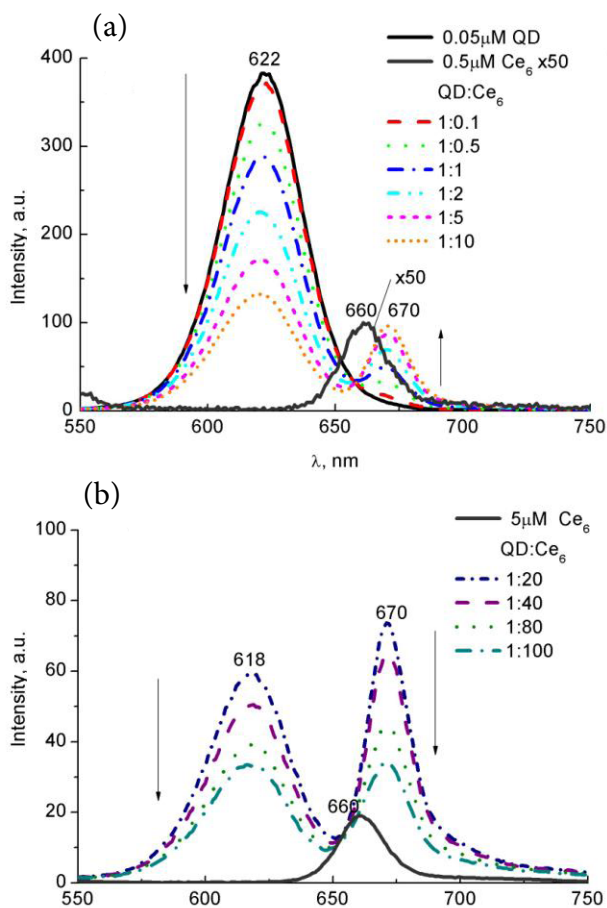


Fig. 2. Fluorescence spectra of QDs,  $Ce_6$  solutions and QD- $Ce_6$  mixture solutions at various QD: $Ce_6$  molar ratios: (a) from 1:0.1 to 1:10, and (b) from 1:20 to 1:100;  $\lambda_{ex} = 465$  nm (fluorescence intensity of free  $Ce_6$  is multiplied by 50).

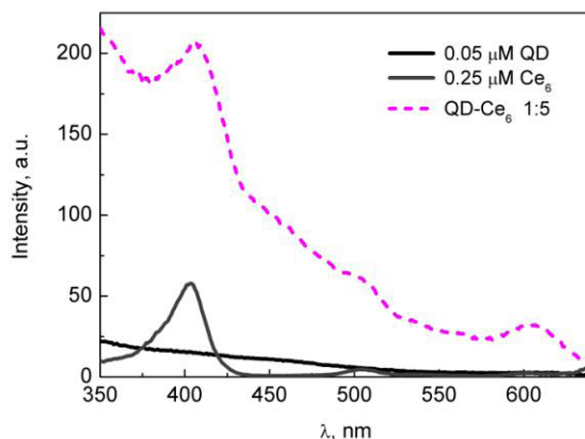


Fig. 3. Fluorescence excitation spectra of 0.05  $\mu$ M QDs, 0.25  $\mu$ M  $Ce_6$  solutions and QD- $Ce_6$  mixture solution at molar ratio 1:5; spectra were recorded at  $\lambda_{em} = 670$  nm.

complex formation. To elucidate the actual origin of QDs and  $Ce_6$  interaction, the fluorescence measurements were performed with identical QDs, only coated with terminal carboxyl (negatively charged) groups replacing amino (positively charged) groups. However, the fluorescence band of  $Ce_6$  underwent a similar bathochromic shift to 670 nm (Fig. 4).

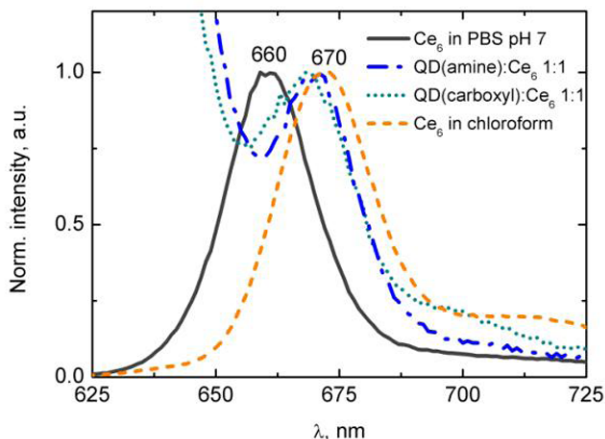


Fig. 4. Normalized fluorescence spectra of  $Ce_6$  in PBS in the presence of QDs with terminal amino or carboxyl groups, and  $Ce_6$  in chloroform.

### 3.2. Formation and stability of QD- $Ce_6$ complex in the presence of BSA

To investigate the formation and stability of a QD- $Ce_6$  complex in the model biological medium, spectroscopic measurements were performed in the presence of bovine serum albumin (BSA).

The addition of BSA to the QDs solution resulted in a negligible quenching of QDs photoluminescence intensity, and no other spectral changes were observed (data not shown). Also, the presence of protein did not change the stability of QDs photoluminescence over time. On the other hand, the addition of BSA induced a bathochromic shift of  $Ce_6$  spectral bands, which is typical of interaction between a tetrapyrrolic compound and protein [10, 11]. A fluorescence band of  $Ce_6$  was also shifted bathochromically to 670 nm, equally as the band of  $Ce_6$  bound to QDs.

Appropriate volumes of  $Ce_6$ , QDs, and BSA stock solutions were added to QD-BSA,  $Ce_6$ -BSA, and QD- $Ce_6$  mixture solutions, respectively, to reach the same final concentrations of solutes.

The emission spectra ( $\lambda_{ex} = 465$  nm) of the first solution (QD-BSA with added  $Ce_6$ ) (Fig. 5(a)) and of the second one ( $Ce_6$ -BSA with added QDs) (Fig. 5(b)) showed the same spectral changes as in

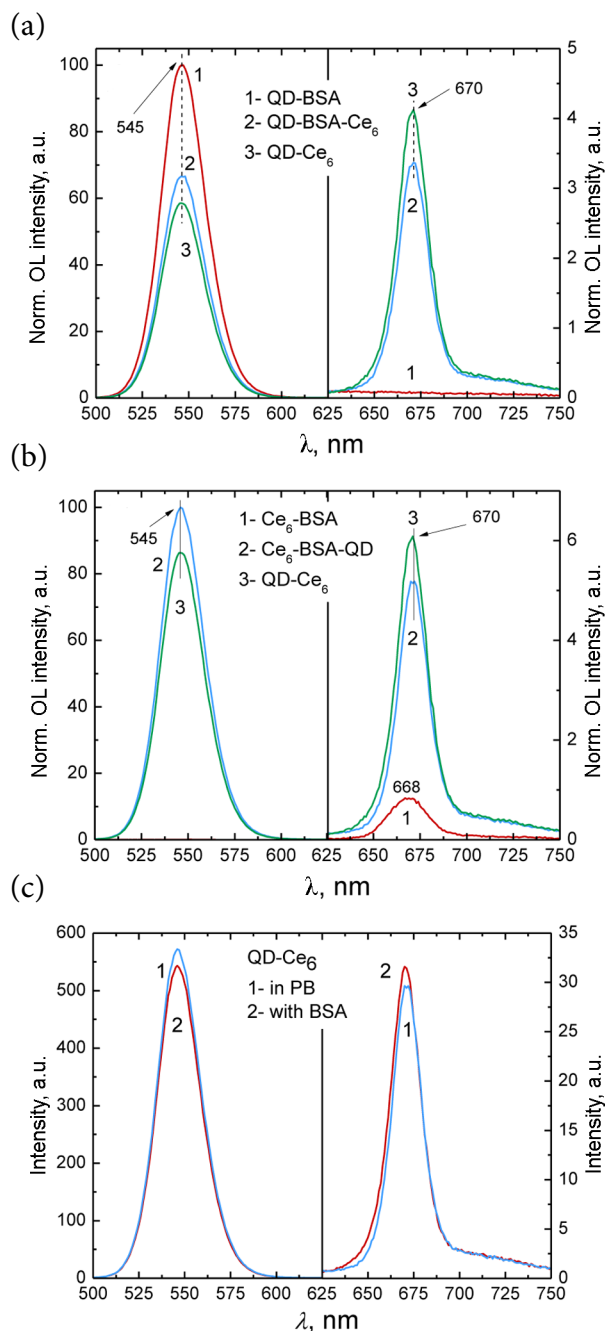


Fig. 5. Normalized emission spectra of (a) QD-BSA ( $0.05 \mu\text{M} : 1 \mu\text{M}$ ) and (b)  $Ce_6$ -BSA ( $0.5 \mu\text{M} : 1 \mu\text{M}$ ) solutions after addition of  $Ce_6$  ( $0.5 \mu\text{M}$ ) and QD ( $0.05 \mu\text{M}$ ), respectively. Emission spectra before addition of  $Ce_6$  and BSA to QD-BSA and  $Ce_6$ -BSA solutions, respectively, are also shown along with QD- $Ce_6$  emission spectra in the absence of protein, (c) QD- $Ce_6$  ( $0.05 \mu\text{M} : 0.5 \mu\text{M}$ ) solution before and after addition of BSA ( $c = 1 \mu\text{M}$ ). Spectra were recorded using  $\lambda_{ex} = 465$  nm.

the case of QD-Ce<sub>6</sub> complex formation in PBS. In all cases photoluminescence intensity of QDs was quenched with simultaneous significant increase in the intensity of the Ce<sub>6</sub> fluorescence band at 670 nm.

However, the intensity of the QDs photoluminescence band was higher and the intensity of fluorescence of bound Ce<sub>6</sub> molecules was lower in the presence of BSA for both cases of mixing order. Similar spectral changes were also obtained for the third solution (QD-Ce<sub>6</sub> with added BSA) (Fig. 5(c)). The results obtained suggest that the presence of BSA does not prevent QD-Ce<sub>6</sub> complex formation, regardless of the primacy of interaction of BSA with QDs or Ce<sub>6</sub> molecules.

### 3.3. Effect of lipid coating on the formation of QD-Ce<sub>6</sub> complex

To elucidate the process of complexation between QDs and Ce<sub>6</sub>, the surface of hydrophobic QDs was modified using three different phospholipids containing saturated and unsaturated fatty acids: DOPC, PEG-DPPE, or PEG-DOPE. While modification with PEG-DPPE or PEG-DOPE resulted in solubility of coated QDs and stability of aqueous colloidal solutions, it was found that QDs covered with DOPC became insoluble. Also, the colloidal solution of QDs modified by the mixture of DOPC:PEG-DPPE (molar ratio 2:1) was unstable. On the other hand, QDs encapsulated into DOPC:PEG-DOPE micelles with molar ratios of 1:1 and 2:1 showed long-term stability in the aqueous solution.

The modification of QD surface with different phospholipids had no effect on the absorption spectrum of QDs in comparison with that in toluene. However, the quantum yield of QDs PL slightly decreased after modification.

The formation of a complex between Ce<sub>6</sub> and superficially modified QDs was tested by adding a small volume of a Ce<sub>6</sub> stock solution to 50 nM solutions of modified QDs to obtain a molar ratio 1:5 for QD:Ce<sub>6</sub>. The addition of Ce<sub>6</sub> to the colloidal solution of QDs covered with PEG-DPPE made no effect on the spectral properties of either QDs or Ce<sub>6</sub> (data not shown). However, the addition of Ce<sub>6</sub> to the colloidal solution of QDs covered with unsaturated phospholipids PEG-DOPE and DOPC:PEG-DOPE resulted in significant spectral

changes of the PL of QDs and Ce<sub>6</sub> (Fig. 6). These experiments revealed that the coating of QDs with phospholipids with unsaturated bonds favours the complexation of Ce<sub>6</sub> with such QDs.

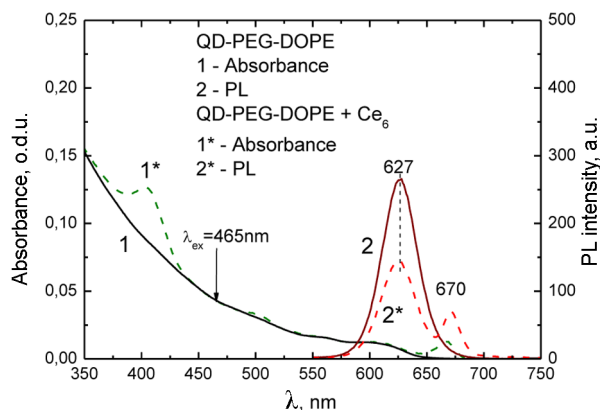


Fig. 6. Absorption and fluorescence spectra of QD-PEG-DOPE and QD-PEG-DOPE+Ce<sub>6</sub> solutions (concentration of Ce<sub>6</sub> was 0.25 μM).

### 3.4. Production of singlet oxygen by QD-Ce<sub>6</sub> complex

Figure 7(a–d) shows the normalized absorption and emission spectra registered in the solutions of QDs, Ce<sub>6</sub>, QD-Ce<sub>6</sub> mixture, and SOSG, which was used for the detection of singlet oxygen.

Complexation with QDs resulted in the shift of the last absorption band of Ce<sub>6</sub> from 655 to 660 nm. The intensity of QDs photoluminescence was quenched to half of its initial value. Excitation at 460 nm of a non-irradiated QD-Ce<sub>6</sub> mixture solution yielded a combined emission spectrum with the peaks at 630 and 670 nm, originated from QDs and from Ce<sub>6</sub> molecules complexed with QDs (Fig. 7(c)). The most intense absorption band of SOSG was at 508 nm and two much weaker bands were at 374 and 395 nm. The fluorescence band of SOSG at 525 nm did not overlap with emission bands of QDs and Ce<sub>6</sub> (Fig. 7(d)).

All solutions were irradiated with a light beam at around 460 nm since the absorbance of Ce<sub>6</sub> at this wavelength is minimal. Thus, the stability of a QD-Ce<sub>6</sub> complex and generation of singlet oxygen were assessed in a way preventing the direct photoexcitation of Ce<sub>6</sub>.

Figure 8(a) shows relative changes in emission intensity of irradiated Ce<sub>6</sub>, QDs, and QD-Ce<sub>6</sub>

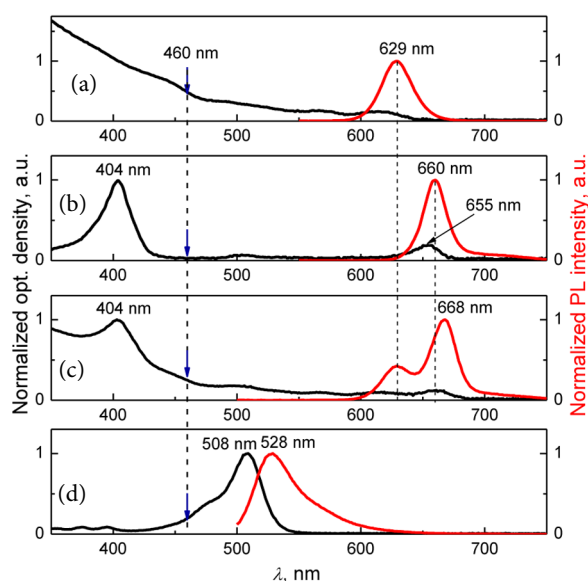


Fig. 7. Normalized absorption and emission spectra of (a)  $0.02 \mu\text{M}$  QDs, (b)  $0.2 \mu\text{M}$   $\text{Ce}_6$ , (c) QD- $\text{Ce}_6$  (QD: $\text{Ce}_6$  1:10), and (d)  $2 \mu\text{M}$  SOSG solutions (PB pH 7). Excitation at 460 nm was used for QDs,  $\text{Ce}_6$  and QD- $\text{Ce}_6$  solutions, while excitation for SOSG solution was at 504 nm. Absorption spectra were normalized at excitation wavelength, while emission was normalized at intensity maximum. Arrows indicate the wavelength of irradiation.

solutions depending on the delivered irradiation dose, which are normalized to the absorbance at an irradiation wavelength (460 nm). Distinct changes in PL bands of QDs at 630 nm and of a QD- $\text{Ce}_6$

complex at 670 nm were detected in the mixture solution in comparison with those in homogenous solutions. The intensity of the band at 670 nm diminished by 90% after exposure to  $128 \text{ J/cm}^2$  while the PL of QDs increased 3.6 times.

Figure 8(b) shows changes in fluorescence intensity of SOSG in QDs,  $\text{Ce}_6$ , and QD- $\text{Ce}_6$  mixture solutions measured at 528 nm after various exposures to the light beam at about 460 nm. A significant increase of SOSG fluorescence intensity for about 30% was observed in QD- $\text{Ce}_6$  mixture after exposure to  $160 \text{ J/cm}^2$ . However, almost no fluorescence changes of SOSG were registered in solutions of QDs and  $\text{Ce}_6$ .

### 3.5. Uptake of QD- $\text{Ce}_6$ complex in cells

The uptake of  $1 \mu\text{M}$   $\text{Ce}_6$ ,  $0.2 \mu\text{M}$  QDs, and QD- $\text{Ce}_6$  complex in MiaPaCa-2 cells was examined using laser confocal microscopy with an accessory for PL lifetime imaging. In order to investigate whether  $\text{Ce}_6$  molecules remain bound to QDs after intracellular uptake, pictures of cells with accumulated  $\text{Ce}_6$ , QDs, and QD- $\text{Ce}_6$  were taken and the fluorescence lifetime measurements were performed in different sites of cells. The obtained data are summarized in Fig. 9.

A typical fluorescence lifetime of  $\text{Ce}_6$  in cells was found to be 5.9 ns and did not vary in membrane and cytoplasm compartments of the cell. While typical PL lifetimes of QDs in plasma membrane and

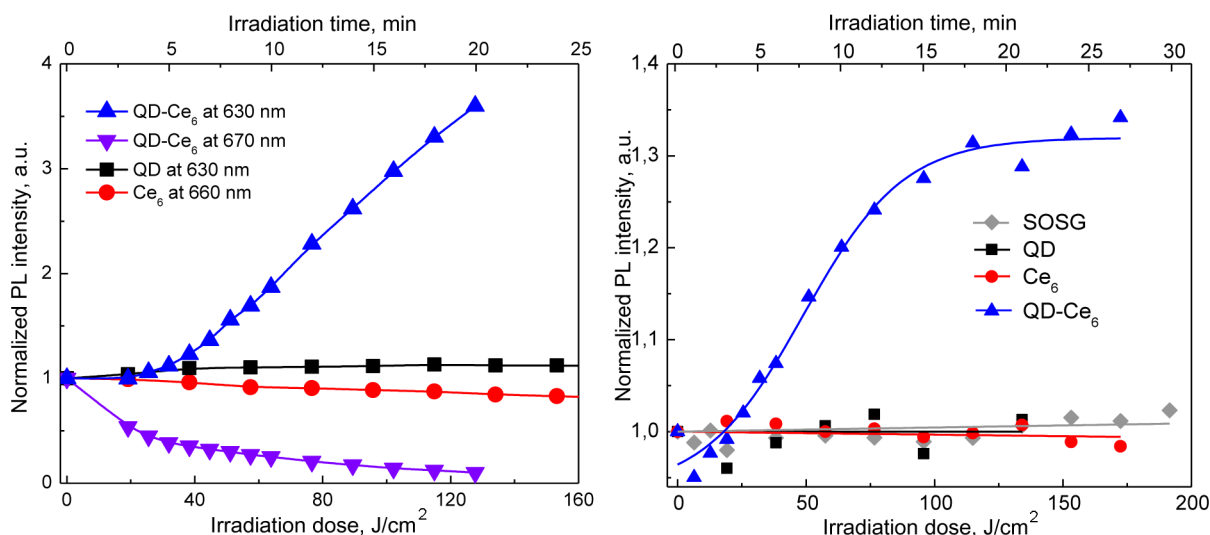


Fig. 8. Changes of photoluminescence of QDs,  $\text{Ce}_6$  and QD- $\text{Ce}_6$  mixture solutions measured at corresponding wavelengths (left panel) and fluorescence of SOSG measured at 528 nm (right panel) after various exposures to light beam at about 460 nm. Intensities were normalized according to formulae  $I_{\text{irr}}/I_{\text{nonirr}} \times A_{\text{nonirr}}/A_{\text{irr}}$ .

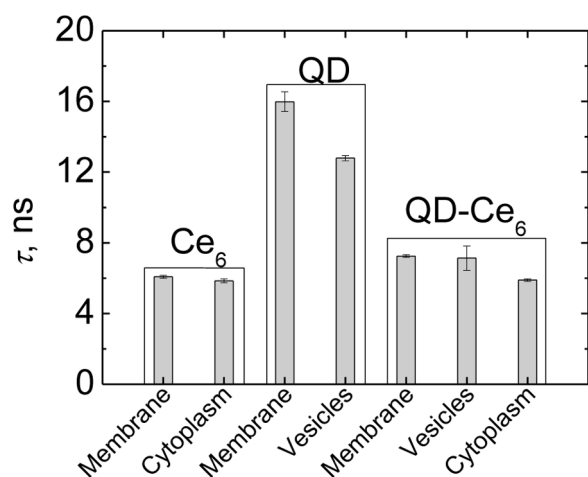


Fig. 9. Averaged fluorescence lifetimes of Ce<sub>6</sub>, QDs and QD-Ce<sub>6</sub> complex in different locations of MiaPaCa-2 cancer cells.

inner vesicles were slightly different, 16 and 12.8 ns, respectively, in the cells incubated with a QD-Ce<sub>6</sub> complex the PL lifetime value of QDs changed to 7.3 ns, which indicated a strong quenching of QDs due to energy transfer to Ce<sub>6</sub>. However, the lifetime measurements in the cytoplasm yielded an averaged PL value of 5.9 ns, which coincided with the PL lifetime value of Ce<sub>6</sub> in cells.

### 3.6. Photosensitizing properties of QD-Ce<sub>6</sub> complex

To determine whether cell incubation with a QD-Ce<sub>6</sub> complex can cause photosensitization and induce photochemical damage upon irradiation, the cells in well plates were exposed to a light dose of 15 J at 470 nm, which is predominantly absorbed by QDs. Following light exposure, the morphology of the MiaPaCa-2 cells incubated with a QD-Ce<sub>6</sub> complex changed dramatically. The phase contrast micros-

copy image (Fig. 10(b)) shows the presence of the randomly shaped, volume-increased cells. These cellular features were not observed in control cells (Fig. 10(a)), indicating possible necrosis and photosensitizing properties of the QD-Ce<sub>6</sub> complex.

## 4. Discussion

Since it was suggested that QDs could be used in the photodynamic therapy of cancer as resonance energy donors for conventional photosensitizers [5], it became clear that the nature of interaction between QDs and photosensitizer molecules would play a very important role in photodynamic processes, affecting stability, photophysical properties and sensitizing effectiveness of such complexes. Spectroscopic investigations of the mixtures of all studied QDs with Ce<sub>6</sub> showed bathochromic shifts of absorption and fluorescence bands of the photosensitizer (Figs. 1, 2), which is typical of micro-environmental changes occurring during complex formation. The fluorescence excitation spectra being registered at the peak of the shifted Ce<sub>6</sub> fluorescence band (Fig. 3) displayed the contribution of both QDs and Ce<sub>6</sub> absorbance confirming that the part of QD energy during photoexcitation was indeed transferred to Ce<sub>6</sub> molecules. Interaction between QDs coated with either positively charged amino groups or negatively charged carboxyl groups and photosensitizer Ce<sub>6</sub> resulted in identical spectral positions of the fluorescence band of the latter (Fig. 4), implying that electrostatic interaction is not responsible for the observed formation of a complex between QDs and Ce<sub>6</sub>. The shifted position of this band in relation to that observed in PBS and its similarity with that of Ce<sub>6</sub> dissolved in chloroform indicate that spectral properties of Ce<sub>6</sub>

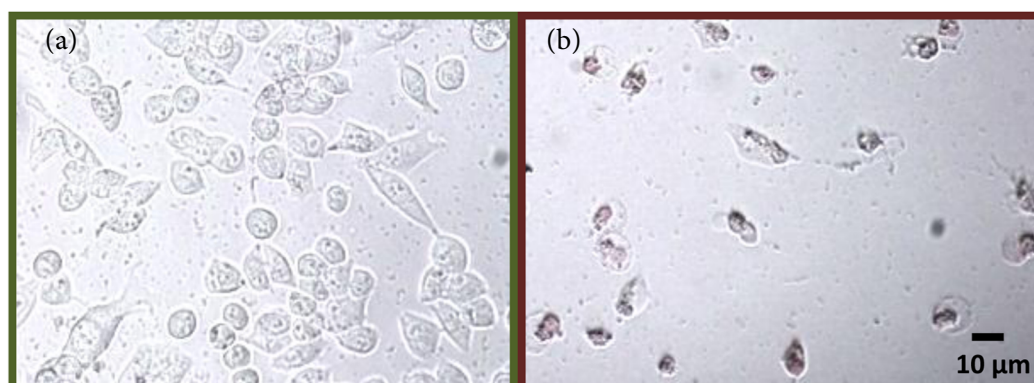


Fig. 10. MiaPaCa-2 - cells (a) after treatment with QD-Ce<sub>6</sub> complex in the dark, and (b) after exposure of 15 J irradiation (470 nm).

are very sensitive to environmental polarity. Since chloroform solution is hydrophobic, it is reasonable to presume that upon binding to QDs,  $Ce_6$  molecules immerse in the hydrophobic part of its lipid coating. This presumption is in agreement with the report, demonstrating the localization of  $Ce_6$  in most cellular membranes [12]. Another study on NMR spectroscopy of  $Ce_6$  also demonstrated its localization in phospholipid bilayers, where  $Ce_6$  was immersed in the vicinity of polar heads of phospholipids [13].

The experiments on the stability of the formed QD- $Ce_6$  complex that were performed in aqueous solutions in the presence of BSA did not reveal any notable changes in the spectral position of the fluorescence band of bound  $Ce_6$  (Fig. 5). The inability of BSA to prevent complex formation irrespective of the mixing sequence of all three components allows presuming that interaction strength between  $Ce_6$  and the molecules of QDs coating is higher than interaction between each of them and BSA taken separately. Nevertheless, a slightly reduced intensity of  $Ce_6$  and increased intensity of QDs PL in the presence of BSA (Fig. 5(a–c)) indicates the involvement of the latter in certain microenvironment changes occurring on QDs surface. It could weaken the affinity of  $Ce_6$  towards QDs, inducing partial complex degradation.

The importance of hydrophobic interactions in the formation of a QD- $Ce_6$  complex was confirmed spectroscopically by conducting experiments with amphiphilic QDs, the surface coating of which had been modified using different phospholipids possessing saturated and unsaturated fatty acids. A notable bathochromic shift of  $Ce_6$  absorption and fluorescence spectra was registered upon mixing PS solution with the solution of QDs coated with unsaturated fatty acid QD-PEG-DOPE (Fig. 6). The indistinguishable similarity of the fluorescence band of  $Ce_6$  at 670 nm with the band of  $Ce_6$  in a QD- $Ce_6$  complex formed in mixture solutions (Fig. 2) confirms the presumption that molecules of  $Ce_6$  interact with the hydrophobic side of phospholipidic coating of QDs and that the presence of unsaturated fatty acids in a lipid coating of QDs greatly promotes complex formation.

It was found that a QD- $Ce_6$  complex is formed when a non-polar part of  $Ce_6$  interacts with the hydrophobic part of QDs phospholipid coating [14, 15],

which is evidenced by a fluorescence band shift from 660 to 670 nm, analogous as for  $Ce_6$  molecules present in the hydrophobic environment [13, 16–18].

Being in close proximity  $Ce_6$  conjugated with a QD could be indirectly excited by FRET from the QD to the sensitizer. Efficient energy transfer from QDs to bound  $Ce_6$  molecules is achieved due to close localization of  $Ce_6$  molecules to the core of QDs which is crucial for its further application in photodynamic therapy of cancer. Due to size dependent PL wavelength the QDs photoluminescence band can be tuned to overlap with the absorption band of PS, therefore exciting one via FRET. The excited PS molecules would act in the same way as in conventional PDT producing active cell destructive species.

Following the studies on application of QD-PS conjugates in PDT, employing QDs as potential energy donors for photosensitizers [5], it was of interest to test the most important requirement for PDT agents – the ability to generate singlet oxygen ( $^1O_2$ ), which is the main reactive intermediate in photosensitized cancer cell killing. The detection of singlet oxygen generated during irradiation of QD- $Ce_6$  solutions was performed using commercially available SOSG.

Irradiation of QD- $Ce_6$  complex solution caused a significant (about 30%) increase in intensity of SOSG fluorescence measured at 528 nm, which is proportional to the detected amount of  $^1O_2$  (Fig. 8(b)). This result indicates that upon irradiation in the region of QDs absorbance,  $^1O_2$  is produced. So, it seems that a QD- $Ce_6$  complex irradiated by visible light is able to produce  $^1O_2$  more efficiently than QDs or  $Ce_6$  alone and be a potential candidate for PDT.

When considering application of a QD- $Ce_6$  complex in PDT, it is very important to ascertain whether weak hydrophobic interaction between PS molecules and QDs is enough to induce cancer cell killing by using the FRET mechanism. The interference of various kinds of biomolecules in cytoplasm with a QD- $Ce_6$  complex may not only weaken its stability, but also enhance nonradiative decays and lead to shortening of the PL lifetime [19] thus creating the concurrence for FRET-based photosensitization. However, comparative PL lifetime imaging measurements performed in the cells (Fig. 9) revealed that the PL lifetime of

QDs in the absence of  $Ce_6$  was 2 times longer than in its presence, confirming intracellular stability of the QD- $Ce_6$  complex as well as FRET occurrence. The observed photoinactivation of cells (Fig. 10) incubated with a QD- $Ce_6$  complex under irradiation in the spectral region minimizing direct excitation of a photosensitizer provided clear evidence for complex capacity to induce FRET-mediated cell eradication.

## 5. Conclusions

Spectroscopic studies on the formation of a non-covalent complex between QDs bearing different coatings and photosensitizer chlorin  $e_6$  in an aqueous medium and in the presence of BSA revealed that the QD- $Ce_6$  complex is driven by hydrophobic interaction between the amphiphilic coating of quantum dots and non-polar moiety of chlorin  $e_6$ . Neither interaction with BSA nor intracellular environment could prevent complex formation; however, slight influence on its stability was observed. An investigation on the capacity of such complex to generate  $^1O_2$  showed that irradiation of the QD- $Ce_6$  complex with visible light, almost completely not absorbed by the sensitizer, produces  $^1O_2$  more efficiently than QDs or  $Ce_6$  being exposed separately, due to effective energy transfer in such complex from QDs to bound chlorin  $e_6$  molecules. The photoinactivation of cells incubated with a QD- $Ce_6$  complex evidenced that such complexes could induce FRET-mediated cell destruction, implying that such complexes could be used to create selective innovative techniques for photodynamic therapy based on biomedical application of femtosecond pulsed laser systems for two-photon excitation of photosensitizers.

## Acknowledgements

This research was supported by the Norwegian Financial Mechanism and the Republic of Lithuania within the project “Multifunctional nanoparticles for specific non-invasive early diagnostics and treatment of cancer” (Contract No. LT0036) and Research Council of Lithuania Grant No. MIP-095/2011). A. S. is grateful for the Lithuanian Science Council Student Research Fellowship Award, and J. V. for the Postdoctoral Fellowship Implementation in Lithuania.

## References

- [1] K.R. Weishaupf, C.J. Gomer, and T.J. Dougherty, Identification of singlet oxygen as the cytotoxic agent in photoinactivation of a murine tumor, *Cancer Res.* **36**, 2326–2329 (1976).
- [2] J.M. Fernandez, M.D. Bilgin, and L.I. Grossweiner, Singlet oxygen generation by photodynamic agents, *J. Photochem. Photobiol. B Biol.* **37**(1–2), 131–140 (1997).
- [3] B. Čunderlikova, L. Gangeskar, and J. Moan, Acid-base properties of chlorin  $e_6$ : relation to cellular uptake, *J. Photochem. Photobiol. B Biol.* **53**(1–3), 81–90 (1999).
- [4] D. Kessel and R.D. Poretz, Sites of photodamage induced by photodynamic therapy with a chlorin  $e_6$  triacetoxymethyl ester (CAME), *Photochem. Photobiol.* **71**, 94–96 (2000).
- [5] A.C.S. Samia, X.B. Chen, and C. Burda, Semiconductor quantum dots for photodynamic therapy, *J. Am. Chem. Soc.* **125**(51), 15736–15737 (2003).
- [6] R. Bakalova, H. Ohba, Z. Zhelev, M. Ishikawa, and Y. Baba, Quantum dots as photosensitizers? *Nat. Biotechnol.* **22**(11), 1360–1361 (2004).
- [7] P. Juzenas, W. Chen, Y.P. Sun, M.A. Coelho, R. Generalov, N. Generalova, and I.L. Christensen, Quantum dots and nanoparticles for photodynamic and radiation therapies of cancer, *Adv. Drug Deliv. Rev.* **60**(15), 1600–1614 (2008).
- [8] E. Yaghini, A.M. Seifalian, and A.J. MacRobert, Quantum dots and their potential biomedical applications in photosensitization for photodynamic therapy, *Nanomedicine* **4**(3), 353–363 (2009).
- [9] L. Shi, B. Hernandez, and M. Selke, Singlet oxygen generation from water-soluble quantum dot-organic dye nanocomposites, *J. Am. Chem. Soc.* **128**, 6278–6279 (2006).
- [10] A. Jasaitis Jr., G. Streckyte, and R. Rotomskis, Photophysics of sensitizer-protein complexes, *Lith. J. Phys.* **36**, 299–302 (1996).
- [11] A.Jr. Jasaitis, G. Streckyte, and R. Rotomskis, Binding of porphyrin-type sensitizers to human serum albumin: spectroscopic investigation, *Biologija* **2**, 16–23 (1997).
- [12] R. Bachor, C.R. Shea, R. Gillies, and T. Hasan, Photosensitized destruction of human bladder-carcinoma cells treated with chlorin  $e_6$ -conjugated microspheres, *Proc. Natl. Acad. Sci. USA* **88**(4), 1580–1584 (1991).
- [13] M. Vermathen, M. Marzorati, P. Vermathen, and P. Bigler, pH-Dependent distribution of chlorin  $e_6$  derivatives across phospholipid bilayers probed by NMR spectroscopy, *Langmuir* **26**(13), 11085–11094 (2010).
- [14] J. Valanciunaite, A. Skripka, R. Araminaite, K. Kalantojus, G. Streckyte, and R. Rotomskis, Spectroscopic study of non-covalent complex

- formation between different porphyrin analogues and quantum dots with lipid-based coating, *Chemija* **22**(4), 181–187 (2011).
- [15] J. Valanciunaite, A. Skripka, G. Streckyte, and R. Rotomskis, Complex of water-soluble CdSe/ZnS quantum dots and chlorine  $e_6$ : interaction and FRET, *Proc. SPIE* **7376**, Laser Applications in Life Sciences, 737607-1 (2010).
- [16] A.A. Frolov, E.I. Zenkevich, G.P. Gurinovich, and G.A. Kochubeyev, Chlorin  $e_6$ -liposome interaction – investigation by the methods of fluorescence spectroscopy and inductive resonance energy-transfer, *J. Photochem. Photobiol. B Biol.* **7**(1), 43–56 (1990).
- [17] H. Mojzisova, S. Bonneau, C. Vever-Bizet, and D. Brault, The pH-dependent distribution of the photosensitizer chlorin  $e_6$  among plasma proteins and membranes: a physico-chemical approach, *Bioch. Biophys. Acta* **1768**, 366–374 (2007).
- [18] Y. Zhang and H. Gorner, Photoprocesses of chlorin  $e_6$  bound to lysozyme or bovin serum albumin, *Dyes Pigments* **83**, 174–179 (2009).
- [19] Y. Zhang, L. Mi, P.N. Wang, S.J. Lu, J.Y. Chen, J. Guo, W.L. Yang, and C.C. Wang, Photoluminescence decay dynamics of thiol-capped CdTe quantum dots in living cells under microexcitation, *Small* **4**(6), 777–780 (2008).

## MODIFIKUOTO PAVIRŠIAUS KVANTINIŲ TAŠKŲ IR CHLORINO $e_6$ KOMPLEKSAI FOTODINAMINEI TERAPIJAI

R. Rotomskis <sup>a,b</sup>, J. Valančiūnaitė <sup>b</sup>, A. Skripka <sup>b</sup>, S. Steponkienė <sup>b</sup>, G. Špogis <sup>b</sup>, S. Bagdonas <sup>a</sup>, G. Streckytė <sup>a</sup>

<sup>a</sup> *Vilniaus universiteto Lazerinių tyrimų centras, Vilnius, Lietuva*

<sup>b</sup> *Vilniaus universiteto Onkologijos institutas, Vilnius, Lietuva*

### Santrauka

Pastaraisiais metais buvo pasiūlyta, kad kvantiniai taškai (KT) galėtų tapti energijos donorais tradiciniams porfirinams, taikomiems vėžio gydymui fotodinaminės terapijos metodu. Šiame darbe spektroskopiniais metodais tirtas nekovalentinės prigimties kompleksas tarp KT ir fotosensibilizatoriaus chlorino  $e_6$  ( $Ce_6$ ) susidarymas vandeninėje terpėje ir jaučio serumo albumino aplinkoje. KT ir  $Ce_6$  sugerties ir fluorescencijos spektrų pokyčiai atskleidė, kad KT ir  $Ce_6$  kompleksas formavimasis vyksta dėl hidrofobinės sąveikos tarp amfifilinio fotosensibilizatoriaus molekulos ne-

polinės dalies ir hidrofobinės KT lipidinio dangalo dalies. Tokiuose kompleksuose fotosensibilizatorius gali būti sužadintas netiesiogiai vykstant Fiersterio rezonansinės energijos pernašai. Švitinamas regimosios šviesos spinduliuote, KT ir  $Ce_6$  kompleksas generuoja singuletinį deguonį aktyviau negu jo atskirai švitinami komponentai. Inkubavus vėžio ląsteles KT ir  $Ce_6$  kompleksu tirpalu ir pašvitinus šviesa, kurios sensibilizatorius nesugeria, didelė dalis ląstelių žuvo. Stabilių KT ir fotosensibilizatorių kompleksų citotoksiškumas ląstelėse galėtų būti panaudotas kuriant selektyvias fotodinaminės terapijos metodikas.